Proteomic Analysis of *Pseudomonas aeruginosa* Grown Under Magnesium Limitation

Tina Guina
Department of Pediatrics, Division of Infectious Diseases, University of Washington, Seattle, Washington, USA

Manhong Wu and Samuel I. Miller
Departments of Microbiology, Medicine, and Genome Sciences, University of Washington, Seattle, Washington, USA

Samuel O. Purvine, Eugene C. Yi, Jimmy Eng, David R. Goodlett, and Ruedi Aebersold
Institute for Systems Biology, Seattle, Washington, USA

Robert K. Ernst
Department of Medicine, Division of Infectious Diseases, University of Washington, Seattle, Washington, USA

Kimberly A. Lee
Department of Biochemistry, University of Washington, Seattle, Washington, USA

In this study, large-scale qualitative and quantitative proteomic technology was applied to the analysis of the opportunistic bacterial pathogen *Pseudomonas aeruginosa* grown under magnesium limitation, an environmental condition previously shown to induce expression of various virulence factors. For quantitative analysis, whole cell and membrane proteins were differentially labeled with isotope-coded affinity tag (ICAT) reagents and ICAT reagent-labeled peptides were separated by two-dimensional chromatography prior to analysis by electrospray ionization-tandem mass spectrometry (ESI-MS/MS) in an ion trap mass spectrometer (ITMS). To increase the number of protein identifications, gas-phase fractionation (GPF) in the *m/z* dimension was employed for analysis of ICAT peptides derived from whole cell extracts. The experiments confirmed expression of 1331 *P. aeruginosa* proteins of which 145 were differentially expressed upon limitation of magnesium. A number of conserved Gram-negative magnesium stress-response proteins involved in bacterial virulence were among the most abundant proteins induced in low magnesium. Comparative ICAT analysis of membrane versus whole cell protein indicated that growth of *P. aeruginosa* in low magnesium resulted in altered subcellular compartmentalization of large enzyme complexes such as ribosomes. This result was confirmed by 2-D PAGE analysis of *P. aeruginosa* outer membrane proteins. This study shows that large-scale quantitative proteomic technology can be successfully applied to the analysis of whole bacteria and to the discovery of functionally relevant biologic phenotypes. (J Am Soc Mass Spectrom 2003, 14, 742–751) © 2003 American Society for Mass Spectrometry

Today, as the genomes of various bacteria have been sequenced, new technologies for genome-wide approaches for analysis of bacterial protein regulation are being explored. These include transcriptional profiling by whole-genome DNA microarrays to analyze bacterial gene expression profiles and quantitative protein profiling. Though transcriptional profiling is relatively quick and easy, mRNA abundance is not always a reliable indicator of corresponding protein abundance [1, 2, 3]. In addition, bacterial RNA is relatively unstable and difficult to purify which might limit the detection of rare transcripts. Since bacterial genomes are relatively small, these organisms are ideal model systems for development and application of proteomic technology. Unlike more conventional proteome analysis by two-dimensional gel electrophoresis (2-D PAGE), automated in-line microcapillary liquid

Published online May 21, 2003

Address reprint requests to Dr. T. Guina, Department of Pediatrics, Division of Infectious Diseases, University of Washington, HSB K-155 Box 357710, Seattle, WA 98195, USA. E-mail: tguina@u.washington.edu

1044-0305/03/$30.00
doi:10.1016/S1044-0305(03)00133-8

Received December 27, 2002
Revised February 11, 2003
Accepted February 11, 2003

chromatography-electrospray ionization-tandem mass spectrometry (μLC-ESI-MS/MS) enhances the possibility for identification of low abundance and membrane proteins [4, 5]. Furthermore, recently developed technology enables protein quantification in the complex mixtures by differential protein labeling using reagents such as isotope-coded affinity tags (ICAT) [6]. Quantitative protein analysis using ICAT is performed by differential stable isotope labeling of proteins via alkylation of cysteinyl residues. This study utilized a combination of proteomic technologies for global analysis of protein expression and regulation in the Gram-negative opportunistic pathogen *P. aeruginosa*.

While not causing disease in healthy individuals, *P. aeruginosa* causes disease in situations in which the immune barrier has been breached, e.g., in skin burns or immunocompromised individuals [7]. Furthermore, chronic *P. aeruginosa* lung infection is a major cause of mortality in patients with cystic fibrosis (CF), the most common genetic disease of Caucasians [8]. Airways of almost 100% of CF patients are infected with *P. aeruginosa* by three years of age [9]. *P. aeruginosa* isolates from CF patients' airway have unique properties that are the result of adaptation of this bacterium to the specific lung environment. One of the earliest reported adaptations of *P. aeruginosa* isolates from airways of infants with CF is the synthesis of specific lipopolysaccharide (LPS) at the bacterial surface. The result of such envelope modification is increased bacterial resistance to antimicrobial peptides [10, 11] and increased proinflammatory signaling through the human Tlr4 receptor [12]. *P. aeruginosa* was also isolated from CF patients' airways in the form of biofilms, antibiotic-resistant bacterial communities [13]. Some of the properties that are characteristic for clinical isolates of *P. aeruginosa*, such as synthesis of CF-specific LPS, can be also induced in vitro by growth of the bacteria in medium limited for magnesium.

In order to define protein expression and regulation in *P. aeruginosa* grown under magnesium stress we utilized qualitative and quantitative proteomic technology. Peptides derived from the *P. aeruginosa* whole cell or membrane fractions were analyzed by μLC-ESI-MS/MS. Genome-wide differences in bacterial protein abundance were determined after differential labeling of *P. aeruginosa* protein with ICAT reagents. Since 87% of the 5570 *P. aeruginosa* predicted open reading frames (ORFs) contain at least one cysteine residue, ICAT reagent-labeling could enable analysis of the majority of the proteome. Examination of several Gram-negative genomes, including those of *P. aeruginosa* and *Salmonella typhimurium* indicated that more than 70% of known and predicted outer membrane proteins (OMPs) of these Gram-negative bacteria do not contain a cysteine (Guina, T., unpublished). Furthermore, a significant number of OMPs are lipoproteins with a sole cysteinyl residue modified by N-acyl diacylglycerol. As a result, most OMPs cannot be labeled by ICAT reagent. To study the regulation of *P. aeruginosa* OMPs during growth in magnesium-limiting conditions, outer membrane protein extracts were separated by 2-D PAGE and selected proteins were identified by matrix-assisted laser desorption ionization-time of flight (MALDI-TOF) peptide fingerprinting.

Experimental

Bacterial Strains and Growth Conditions

P. aeruginosa PAO-1 was obtained from Stephen Lory (Harvard Medical School). PQS-null mutant (PAO-1 PA0999 [6]) was a gift of David D'Argenio (University of Washington). *P. aeruginosa* was grown at 37 °C with aeration (200 rpm) in N-medium [14] supplemented with 38 mM glycerol, 0.1% casamino acids and either 8 μM or 1 mM $MgCl_2$.

Qualitative and Quantitative Proteomic Analysis of Complex Peptide Mixtures

Bacteria were harvested for protein labeling in the late logarithmic phase of growth. Bacterial cells were sedimented at 10,000 $\times$ *g* for 15 min at 4 °C, resuspended in 1:100 volume of 50 mM Tris pH 8.3, 5 mM EDTA (buffer A), frozen in a dry ice-ethanol bath and stored at −80 °C. Once thawed, cells were broken by sonication in an ice water bath. Unbroken cells were removed by sedimentation at 5000 $\times$ *g* for 15 min at 4 °C. A portion of the bacterial cell extract was sedimented further at 120,000 $\times$ *g* for 1 h at 4 °C to pellet insoluble membrane fraction. Membrane proteins were homogenized in ice-cold buffer A. For quantitative protein analysis, 2.5 mg of whole cell or 400 μg of membrane protein was denatured by boiling for 5 min in buffer A containing 0.25% (vol/vol) SDS, cooled to room temperature, diluted 5-fold in buffer A and then reduced with 5 mM tributylphosphine. Denatured and reduced protein was labeled with dO- or d8-ICAT reagent (Applied Biosystems, Foster City, CA) (approximately 0.5 nmol ICAT/μg of protein) for 2.5 h at room temperature. Pair samples were then combined, octylglucoside was added to 0.5% (vol/vol) final concentration and protein was digested with trypsin (1:50 wt/wt trypsin:protein ratio) at 37 °C overnight. Tryptic peptides were separated by cation exchange (SCX) chromatography on a PolySULFOETHYL A column (2.1 mm $\times$ 20 cm, 5 μM particles, 300 Å pore size; PolyLC Inc., Columbia, MD) used with a Shimadzu (Columbia, MD) LC-10AD VP Liquid Chromatography System. A binary gradient from 10% Buffer B to 40% Buffer B was applied over one h (Buffer A: 10 mM K_2HPO_4, 25% acetonitrile, pH 3.0; Buffer B: 350 mM KCl, 10 mM K_2HPO_4, 25% acetonitrile, pH 3.0). ICAT-labeled peptides were then purified by affinity chromatography of each SCX fraction using Ultralink monomeric avidin (Pierce Biotechnology Inc., Rockford, IL) [5]. ICAT-peptides were finally analyzed by μLC-ESI-MS/MS. Peptides were separated by reversed-phase chromatography using a 100 μm x 10 cm

self-packed Magic C18AQ (Michrom BioResources, Inc., Auburn, CA) column at a flow rate of 250 nl/min. Peptide fragmentation by collision-induced dissociation (CID) was carried out in an automated fashion using the dynamic-exclusion option on a ThermoFinnigan (San Jose, CA) LCQ ion trap mass spectrometer. Each peptide fraction derived from the ICAT-labeled whole cell protein extract was analyzed twice, first from the full *m/z* range (i.e., ion selection for CID from 400–1800 *m/z*) and second by a gas phase fractionation (GPF) protocol [1] in which three overlapping *m/z* windows between 400 and 1800 were used for precursor ion scanning. ICAT-labeled peptides derived from the membrane fraction were analyzed in the full *m/z* range only.

For qualitative protein expression analysis, 200 μg of non-labeled whole cell or membrane protein was denatured and digested by trypsin as mentioned above. Tryptic peptides were purified using PolyHYDROXYETHYL A macro spin columns (PolyLC Inc., Columbia, MD) in 50 mM increments of KCl ranging from 50 to 350 mM (Buffer A: 10 mM K_2HPO_4, 25% acetonitrile, pH 3.0; Buffer B: 350 mM KCl, 10 mM K_2HPO_4, 25% acetonitrile, pH 3.0). Peptide fractions eluting between 50 and 350 mM were analyzed by μLC-ESI-MS/MS as above. Each peptide fraction was analyzed twice, first applying a full *m/z* range (300–1800 *m/z* precursor ion scan) and then the analysis by gas phase fractionation protocol [15] in which five overlapping *m/z* windows between 300 and 1800 were used for precursor ion scanning.

Automated data processing for protein identification and quantification was achieved utilizing SEQUEST and XPRESS software tools [5]. Uninterpreted tandem mass spectra were searched against the *P. aeruginosa* database (http://www.pseudomonas.com). Peptides that showed SEQUEST scores >1.5 were further analyzed manually by detailed spectral analysis as described [5]. Protein abundance ratios larger than +1.5 or smaller than −1.5 were set as a threshold indicating significant changes based on the distribution of values for all proteins quantified in this study and on the assessment of the data variation and reproducibility in several previous studies that utilized ICAT approach to large-scale proteomic analysis [1]. Therefore, relative peptide abundance ratios between −1.5 and +1.5 were considered to represent the steady-state [1, 16].

Isolation of Bacterial Outer Membranes and OMP Analysis by 2-D PAGE-MALDI-TOF Peptide Fingerprinting

P. aeruginosa outer membranes were isolated as previously described [17]. Cultures were grown as described above until late log phase when cells were collected by centrifugation at 8000 × *g* for 15 min at 4 °C. Bacterial spheroplasts were generated by cold osmotic shock in 0.5 M sucrose 10 mM Tris-Cl (pH 7.8) and 60 μg of lysozyme per ml and by subsequent addition of an equal volume of ice-cold 1 μM EDTA. Spheroplasts were broken by French press at 16,000 lb/in^2, unbroken cells were removed by centrifugation at 6000 × *g* for 15 min at 4 °C, and the bacterial extract was separated into fractions by centrifugation at 200,000 × *g* for 1 h at 4 °C. The pellet fraction containing total bacterial membranes was homogenized in 20% sucrose and subjected to sucrose density gradient centrifugation at 180,000 × *g* for 12 to 16 h at 4 °C. The outer membrane fraction was separated as the band of highest buoyant density in the sucrose gradient.

For more efficient protein separation by isoelectric focusing (IEF), aliquots containing 400 μg (for acidic protein separation) or 250 μg (for basic protein separation) total OMP were washed in deionized water and solubilized by boiling for 10 min in 1% (wt/vol) sodium dodecyl sulfate (SDS). Protein was subsequently precipitated in 10 volumes of ice-cold acetone. Removal of the bulk of the outer membrane lipid and LPS aggregates by this technique significantly improved protein separation by IEF. The protein precipitate was resuspended in solubilization buffer containing 9 M urea, 2% Triton X-100, 2% Pharmalyte pH 3–10 (Pharmacia), 2% β-mercaptoethanol, and the protease inhibitors pepstatin (2 μg/ml), aprotinin (2μg/ml), and leupeptin (2 μg/ml). After 2 h of incubation at 37 °C, insoluble material was removed by sedimentation at 14,000 × *g* for 10 min at room temperature. Solubilized protein was first separated by IEF using a Pharmacia Multiphor II electrophoresis unit with immobilized pH gradients (pH 4–7 and pH 6–11) and then on SDS 12% polyacrylamide gels. Protein spots were visualized by staining with Coomassie brilliant blue. Gels were scanned using an UMAX Astra 1200S scanner, and two-dimensional (2-D) profiles of outer membrane proteomes were visually compared. After side-by-side comparison of the protein profiles, protein spots that were regulated by growth in varying magnesium concentrations were excised from Coomassie-stained 2-D SDS-polyacrylamide gels and digested in situ with trypsin as described [17]. Peptides were analyzed by MALDI-TOF and *P. aeruginosa* proteins identified using MS-Fit (Baker, P. R. and Clauser, K. R.; http://prospector.ucsf.edu).

Analysis of Pseudomonas Quinolone Signal (PQS) Production

P. aeruginosa PAO-1 was grown overnight at 37 °C in N-medium supplemented with either 8 μM or 1 mM $MgSO_4$. PQS was extracted from bacterial cultures by acidified ethyl acetate as described [18, 19] and separated on TLC plates (20 × 20 cm silica gel 60 F_{254}; EM Science). Culture extracts were separated with the 17:2:1 methylene chloride/acetonitrile/dioxane solvent. Plates were then air-dried and PQS spots were visualized and photographed under UV light. Photographs were analyzed using the public domain ImageJ pro-

gram (developed at the U.S. National Institutes of Health and available on the Internet at http://rsb.info.nih.gov/ij) to determine relative amounts of PQS.

Results and Discussion

Proteomic Analysis Defined 145 P. aeruginosa Proteins Regulated During Growth Under Magnesium-Limiting Condition

Qualitative and quantitative proteomic approaches were utilized to determine the whole cell and envelope proteome during growth of the Gram-negative bacterial pathogen *P. aeruginosa* in varying magnesium concentrations [growth in presence of low (8 μM) versus growth in high (1 mM) magnesium]. Quantitative proteomic analysis of *P. aeruginosa* was performed via differential labeling of proteins with ICAT reagents [6]. Protein identification and quantification were achieved in silico as previously described [5]. High *P. aeruginosa* proteome coverage was achieved by combination of 2-D chromatographic separation of tryptic peptides followed by gas-phase fractionation (GPF) [15] during LC-ESI-MS/MS analysis. Whole-cell or membrane-derived tryptic peptides were first fractionated by strong cation exchange chromatography and ICAT-labeled peptides were then isolated by avidin chromatography and resulting mixtures were analyzed by reverse phase μLC-ESI-MS/MS (see Methods). For the purpose of selecting ions for CID using data-dependent (DD) instrument control methods, mass spectrometric survey scans are usually carried out across a wide *m/z* range (e.g., 400–1800 *m/z*). However, we utilized GPF, defined here as iterative mass spectrometric ion selection from narrow overlapping *m/z* ranges, to achieve higher proteome coverage from an unfractionated complex mixture of peptides [15] (see Methods). The GPF analysis of ICAT reagent-labeled peptides derived from a whole cell lysate using three overlapping *m/z* ranges that in total covered 400–1800 *m/z* produced 30% more identifications than ion selection from only a single *m/z* window (data not shown).

DNA-microarray transcriptional profiling defined approximately 2250 *P. aeruginosa* ORFs as transcribed during growth in low and high magnesium suggesting that 40% of the potential *P. aeruginosa* proteome is expressed under these conditions. Of these genes, 681 (~30%) were regulated by growth in 8 μM Mg^{2+}, a ratio similar to that found in this proteomic study. 1331 proteins representing 59% of the expressed *P. aeruginosa* proteome as estimated from transcriptional profiling were detected in low and high magnesium growth conditions using both qualitative and quantitative proteomic analysis. The relative abundance of 546 proteins, of which 486 were from whole cell and 163 from the membrane fraction, was determined by quantitative analysis (Table 1 and data not shown). This analysis defined 145 magnesium stress-response proteins of which 76 proteins were induced and 69 proteins were repressed upon growth in low magnesium (not shown). Regulated proteins included 34 metabolic enzymes, 31 putative enzymes, 37 other previously characterized proteins and 43 hypothetical proteins (data not shown). Relative protein abundance ratios (induction and repression) were higher than 2.5-fold for 44 proteins (average standard deviation, average SD 0.42); 29 proteins had abundance ratios indicating change between 2.0- to 2.5-fold (average SD 0.22) and 73 proteins had abundance ratios indicating 1.5- to 2.0-fold changes (average SD 0.13). The overlap between transcriptional profiling and proteomic analysis results regarding the regulatory state (i.e., induction or repression) has been indicated for 23 regulated proteins among which were four conserved magnesium stress-response proteins (Table 2, Figure 3, and data not shown). However, relative expression of 40 proteins appeared to be at the steady-state level (relative abundance −1.5 to +1.5) when *P. aeruginosa* was grown in low magnesium though transcriptional profiling results indicated that expression of the corresponding genes was regulated (data not shown). These results further demonstrate the necessity to integrate transcriptional profiling and proteomic analysis results to better define global regulatory networks.

Table 1. Results of *P. aeruginosa* whole cell and membrane fraction ICAT analysis

	SCX[a]	n-GPF[b]	Tot pep[c]	U-pep[d]	Tot prot[e]
Whole cell	22	3	2496	706	486
Membrane	12	1	755	221	163

[a]Number of cation exchange fractions analyzed by μLC-ESI-MS/MS.
[b]Number of gas-phase fractions or overlapping *m/z* windows applied to the analysis of each SCX fraction.
[c]Total number of identified ICAT-peptides.
[d]Number of unique ICAT-peptide identifications.
[e]Total number of unique protein identifications.

Quantitative Proteomic Analysis Defined P. aeruginosa Virulence Proteins That Were Regulated by Magnesium Limitation

A number of conserved Gram-negative magnesium stress-response proteins involved in bacterial virulence were among the proteins highly induced in low magnesium (Table 2). These included the transcriptional regulator PhoP and magnesium transporter homologue MgtA (Table 2). PhoP orthologues regulate expression of genes essential for virulence and magnesium acquisition in several Gram-negative bacteria [14, 20, 11]. Some of the PhoP-induced enzymes promote increased bacterial resistance to antimicrobial peptides, a key component of host's innate immunity [10, 17, 21, 22]. For example, PhoP-activated LPS modifications, including the addition of aminoarabinose and palmitate to lipid A, promote resistance to the antibiotic polymyxin and other cationic antimicrobial peptides [10, 21, 23]. Consistent with the addition of aminoarabinose to LPS, homologues

Table 2. Selected proteins differentially expressed in *P. aeruginosa* during growth in low magnesium

Gene number	Protein	*n*[a]	u-ICAT[b]	Fold abundance[c]	SD[d]
Conserved magnesium stress response					
1179	two-component response regulator PhoP**	6	1	10.34	0.96
3552	conserved hypothetical protein, PmrH homologue**	7	1	2.84	0.25
3553	probable glycosyl transferase, PmrF homologue	1	1	2.33	na[e]
3554	conserved hypothetical protein, PmrI homologue	34	7	6.09	1.16
4635	conserved hypothetical protein, MgtC homologue**	13	1	3.99	0.56
4825	magnesium transport ATPase MgtA**	85	3	5.80	1.75
Quorum sensing and adaptation					
0934	GTP pyrophosphokinase RelA	2	1	1.53	0.00
0996	probable coenzyme A ligase	1	1	1.57	na
0997	hypothetical protein	16	2	1.57	0.26
0998	hypothetical protein	6	2	2.04	0.24
0999	3-oxoacyl-[acyl-carrier-protein] synthase III FabHI	4	1	1.63	0.14
1432	autoinducer synthesis protein LasI	2	1	3.10	0.05
Secreted factors					
3478	rhamnosyltransferase chain B RhlB	4	1	−1.57	0.15
1899 or 4210*	probable phenazine biosynthesis protein PhzA**	2	2	−2.69	0.00
1900	probable phenazine biosynthesis protein PhzB	8	2	−1.70	0.10
1903 or 4214*	phenazine biosynthesis protein PhzE**	1	1	−2.70	na
1904 or 4215*	probable phenazine biosynthesis protein PhzF**	2	1	−1.85	0.01
4211	probable phenazine biosynthesis protein PhzB	2	1	−1.93	0.07
4224	hypothetical protein PchG	21	2	−5.23	0.25
4225	pyochelin synthetase PchF**	4	3	−1.97	0.14
4226	dihydroaeruginoic acid synthetase PchE**	15	3	−4.23	0.19
4228	pyochelin biosynthesis protein PchD**	30	5	−4.07	0.19
4230	salicylate biosynthesis protein PchB**	17	2	−4.42	0.36
4231	salicylate biosynthesis isochorismate synthase PchA**	1	1	−2.21	na

[a]Total number of independent peptide identifications and quantification events for each protein obtained during μLC-ESI-MS/MS analysis.
[b]Number of unique peptide sequences identified for each protein.
[c]Average ratios of all quantified peptides for each protein representing fold increase in protein abundance during growth of *P. aeruginosa* in 8 μM Mg^{2+}.
[d]Standard deviation calculated from the average fold abundance of all quantified peptides (*n*).
[e]Not applicable. Positive values represent increased relative abundance upon growth in low magnesium; negative values represent decreased relative abundance.
*Identified peptides are identical in both proteins.
**Transcriptional profiling analysis determined that expression of corresponding genes was regulated (i.e., induced or repressed) in a similar fashion.

of *S. enterica* enzymes necessary for aminoarabinose addition and resistance to polymyxin (PA3552–3554) were among the most highly induced proteins in this study (Table 2). These results provide a strong functional correlation between LPS modification enzyme levels and the LPS structural modifications seen in this environmental condition, confirming the validity of ICAT analysis.

A number of *P. aeruginosa* virulence factors are regulated by quorum sensing bacterial communication via small molecule signals *N*-(3-oxododecanoyl)-L-homoserine lactone (3OC12-HSL) and *N*-butyryl-L-homoserine lactone (C4-HSL) [24, 25, 26, 13]. The quantitative protein profiles indicated that magnesium limitation induced several quorum sensing proteins including the 3OC12-HSL synthase LasI [27] and the starvation and general stress-response regulator RelA [28, 29] (Table 2). Furthermore, proteins regulated by quorum sensing such as rhamnosyltransferase and enzymes of both *P. aeruginosa* phenazine antibiotic biosynthesis operons were repressed during growth in low magnesium (Table 2). Recently, a non-HSL *P. aeruginosa* intercellular signal, 2-heptyl 3-hydroxy 4-quinolone (PQS, *Pseudomonas* quinolone signal), a component of the *P. aeruginosa* quorum sensing hierarchy, has been described [19]. A chromosomal region encoding five proteins (PA0996–1000) was recently shown to be essential for the production of PQS [30, 31]. Four proteins encoded by this operon (PA0996–PA0999) were synthesized at increased levels when *P. aeruginosa* was grown in low magnesium (Table 2 and Figure 1). This result suggested that levels of PQS could be increased by growth in low magnesium. In order to test this hypothesis, PQS produced by *P. aeruginosa* was extracted and analyzed by thin-layer chromatography. The amount of PQS was increased approximately 5-fold when *P. aeruginosa* was grown in medium of low magnesium concentration (Figure 2). This result provided strong correlation between synthesis of PQS and abundance of proteins essential for its production. Though proteins essential for PQS production were induced only about 1.5- to 2-fold during *P. aeruginosa* growth under magnesium limitation (Table 2), this resulted in a significant increase in the amount of PQS produced when bacteria were grown in presence of low magnesium (Figure 2). These results suggested that even for the magnesium-regulated proteins that show relatively modest change in

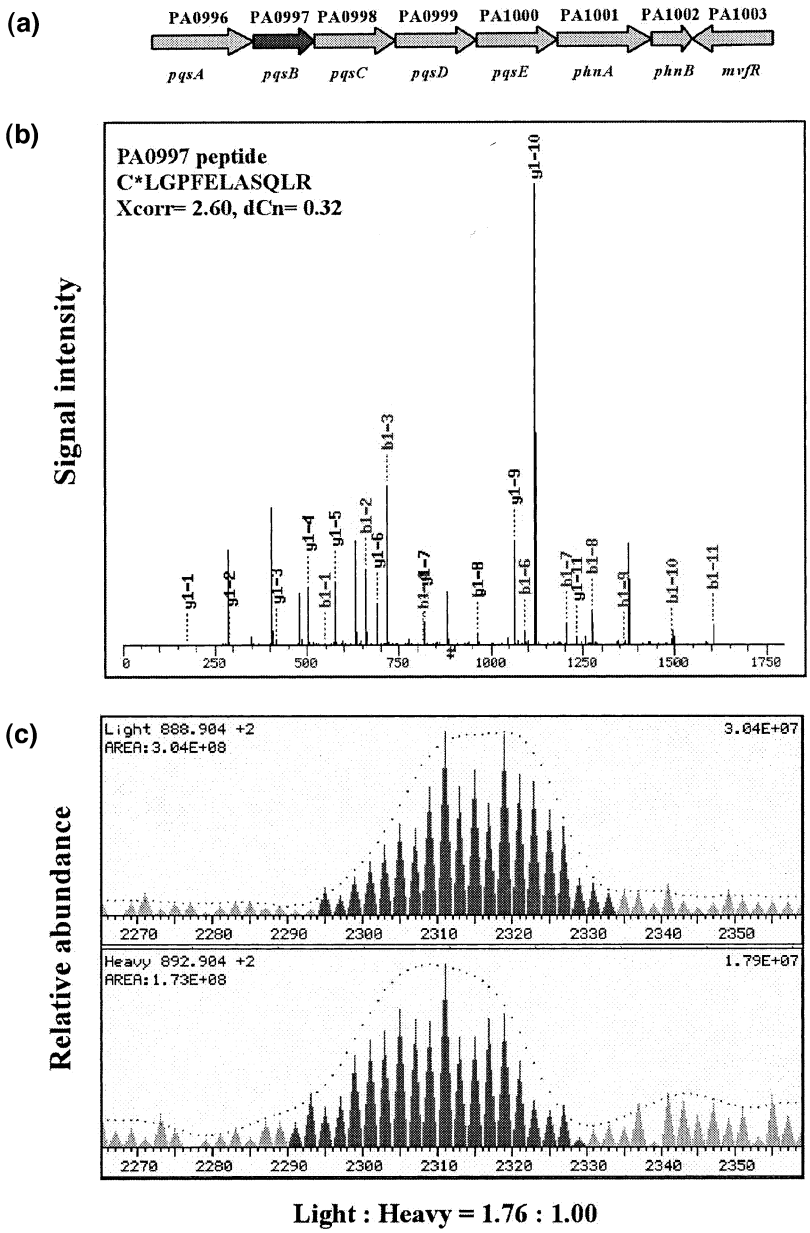

Figure 1. An example of peptide identification and relative abundance quantification of a PQS biosynthesis enzyme PA0997 (PqsB) upon growth of *P. aeruginosa* under magnesium stress. (**a**) Schematic representation of *P. aeruginosa* operon encoding enzymes essential for PQS biosynthesis. (**b**) Tandem mass spectrum of a peptide C*LGPFELASQLR derived from PA0997 (PqsB). *C designates cysteine labeled with the heavy (d8) form of ICAT reagent. Peptide fragment ions of *y* and *b* series that show high correlation and delta correlation scores (Xcorr and dCn, respectively) to the SEQUEST-predicted fragmentation ions of peptide C*LGPFELASQLR are indicated. (**c**) Data indicating the relative abundance and the calculated d0 (Light) to d8 (Heavy) ratio obtained using XPRESS software.

their relative abundance (1.5- to 2.0-fold change), the shift in the abundance was likely biologically significant.

Proteomic Analysis Revealed That Twenty P. aeruginosa Proteins Were Shifting Subcellular Compartment During Bacterial Growth in Magnesium-Limited Medium

Significant Gram-negative envelope remodeling is part of bacterial adaptation to magnesium limitation [10, 23, 11]. To define proteins that contribute to the envelope remodeling either structurally or by providing an enzymatic function to this process by mediating LPS modifications, total membrane protein of *P. aeruginosa* was also analyzed by quantitative proteomic analysis. In this experiment, relative abundance of 163 *P. aeruginosa* proteins during growth in varying magnesium concentrations was determined. 70 of these proteins were induced, and 16 were repressed in the membrane fraction when *P. aeruginosa* was grown in low magne-

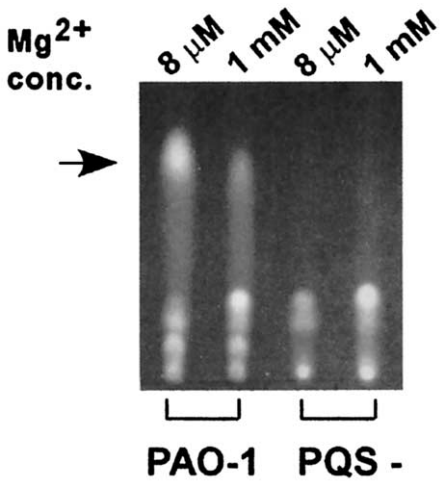

Figure 2. PQS production by *P. aeruginosa*. PQS produced by wild type PAO-1 and a PQS-null mutant (PQS -; a transposon insertion into ORF PA0999 [30]) grown in N-minimal medium containing either 8 μM or 1 mM Mg^{2+}.

sium. Abundance ratios of 106 of membrane-associated proteins were also determined by ICAT analysis of the whole cell protein as described above. Nineteen proteins that were apparently induced at the membrane were also found to be at the steady-state levels (relative abundance ratios of −1.5 to +1.5) when whole cell protein was analyzed (Table 3). These results suggested that although the overall cellular concentration of these 19 proteins remained constant, they were more concentrated at the membrane during growth in low magnesium. In addition, though the cellular concentration of the heat shock chaperone GroEL was reduced by growth in low magnesium, GroEL level was unchanged at the membrane (Table 3). In contrast, relative abundance of protein PA2069 was decreased at the membrane when compared to its concentration in the whole cell during growth in low magnesium. These results suggest that increased abundance of these 21 proteins at the membrane fraction is not a result of increase in transcription of the corresponding genes or protein regulation by posttranslational processing. Instead, changes in protein abundance ratios at the membrane

Table 3. Differential *P. aeruginosa* protein fractionation upon growth in low magnesium

		Membrane protein quantification				Whole cell protein quantification				
Gene number	Protein	*n*[a]	u-ICAT[b]	Fold abundance[c]	SD[d]	*n*	u-ICAT	Fold abundance	SD	M/WC abundance ratio[e]
Energy metabolism										
1583	succinate dehydrogenase (A subunit) SdhA	3	2	2.24	0.40	25	4	1.36	0.22	1.65
1584	succinate dehydrogenase (B subunit) SdhB	7	3	2.20	0.28	2	1	−1.14	0.09	2.50
1585	2-oxoglutarate dehydrogenase (E1 subunit) SucA	10	3	2.97	0.59	9	1	1.04	0.03	2.90
1770	phosphoenolpyruvate synthase PpsA	6	1	3.41	1.07	40	3	1.12	0.23	3.04
5300	cytochrome c5	5	1	2.18	0.17	5	1	1.43	0.11	1.52
5554	ATP synthase beta chain	4	1	1.74	0.18	45	1	1.14	0.13	1.53
5555	ATP synthase gamma chain	2	1	1.98	0.03	11	1	1.33	0.08	1.48
5556	ATP synthase alpha chain	4	1	2.00	0.32	45	1	1.47	0.12	1.36
5557	ATP synthase delta chain	5	1	2.15	0.08	5	1	1.17	0.17	1.84
Translation										
3656	30S ribosomal protein S2	6	1	2.01	0.32	15	1	1.27	0.05	1.58
4239	30S ribosomal protein S4	9	2	2.19	0.22	70	6	1.43	0.28	1.53
4241	30S ribosomal protein S13	5	1	2.42	0.05	74	3	1.32	0.23	1.83
4246	30S ribosomal protein S5	6	1	2.18	0.24	60	1	1.46	0.16	1.50
2071	elongation factor G	2	1	2.17	0.30	11	1	1.29	0.12	1.68
4266	elongation factor G	9	1	2.41	0.22	21	2	1.21	0.11	1.99
Other										
4385	GroEL protein	3	1	−1.16	0.02	3	1	−3.03	0.64	2.61
2991	soluble pyridine nucleotide transhydrogenase	1	1	1.64	na	3	1	1.00	0.05	1.64
4670	ribose-phosphate pyrophosphokinase	23	2	2.13	0.22	10	2	1.31	0.12	1.63
3068	conserved hypothetical protein	1	1	2.13	na	6	1	1.01	0.05	2.11
3263	conserved hypothetical protein	3	1	1.66	0.10	1	1	1.06	na	1.56
2069	probable carbamoyl transferase	3	1	−9.09	0.18	2	2	−1.06	0.13	−8.58

[a]Total number of independent peptide identifications and quantification events for each protein obtained during μLC-ESI-MS/MS analysis.
[b]Number of unique peptide sequences identified for each protein.
[c]Average ratios of all quantified peptides for each protein representing fold increase in protein abundance during growth of *P. aeruginosa* in 8 μM Mg^{2+}.
[d]Standard deviation calculated from the average fold abundance of all quantified peptides (*n*).
[e]Ratio of relative protein abundances determined upon ICAT analysis of membrane fraction and ICAT analysis of whole cell protein. Positive values represent increased relative abundance upon growth in low magnesium; negative values represent decreased relative abundance.

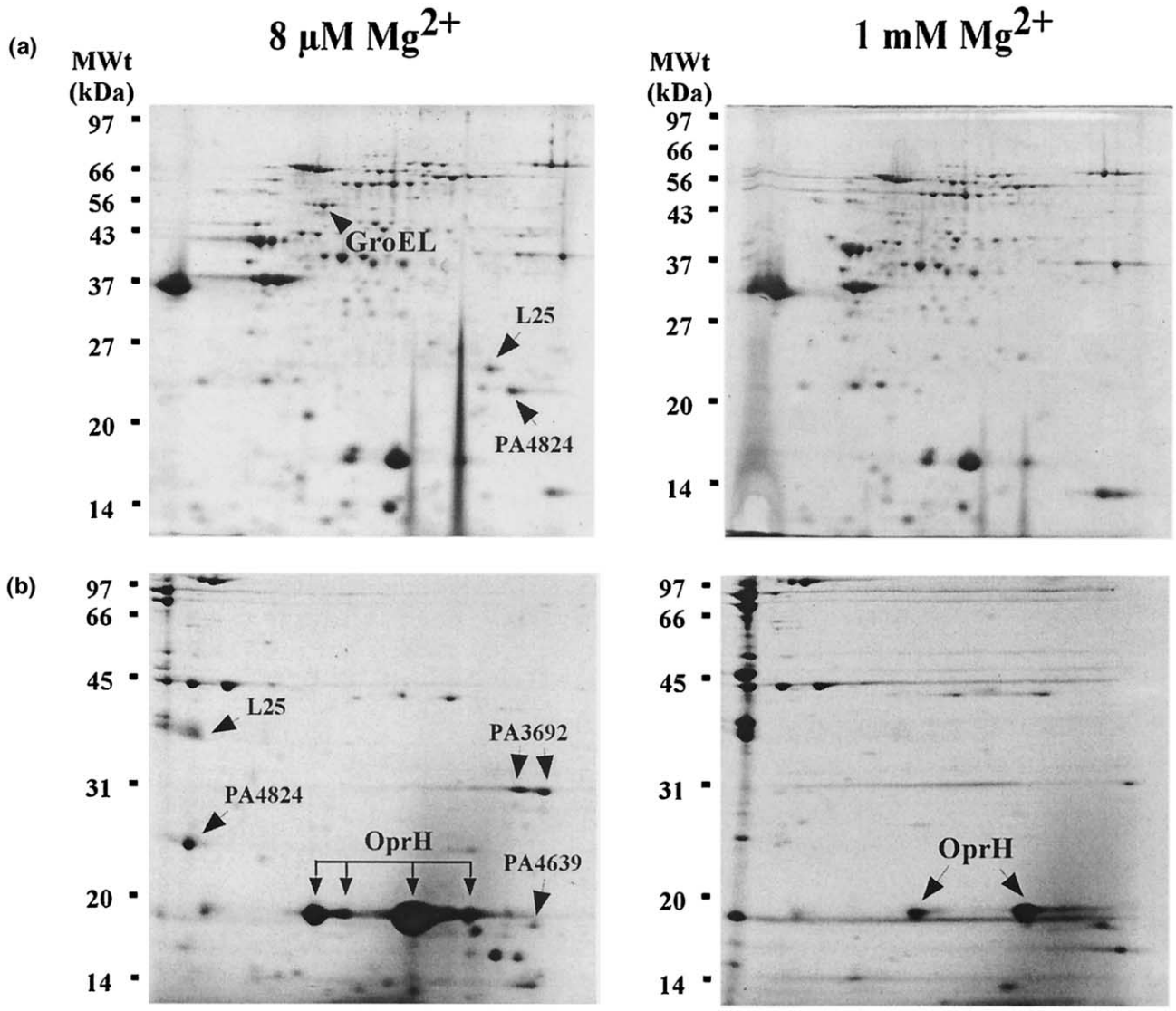

Figure 3. 2-D PAGE map of magnesium-regulated *P. aeruginosa* OMPs. OMPs were isolated from *P. aeruginosa* grown in presence of 8 μM or 1 mM magnesium and separated by IEF on a linear pH gradient and on SDS-12% PAGE gels. Proteins were visualized by staining in Coomassie brilliant blue. Arrows point to *P. aeruginosa* OMPs induced by growth in low magnesium. (**a**) OMPs were separated on a pH 4 to 7 gradient. (**b**) OMPs were separated on a pH 6 to 11 gradient.

reflected changes in their increased subcellular compartmentalization at the envelope during growth of *P. aeruginosa* in magnesium-limiting condition. Nine of these proteins are soluble components of large membrane-associated enzyme complexes participating in energy metabolism pathways, while six proteins are components of the protein translation machinery. Therefore, quantitative proteomic profiling can successfully detect redistribution of protein within the cell.

Since the majority of *P. aeruginosa* outer membrane proteins (OMPs) could not be labeled with ICAT, OMPs regulated during growth in low magnesium were defined by 2-D PAGE and MALDI-TOF peptide mass fingerprinting of purified outer membrane fractions. Results of this analysis showed that six *P. aeruginosa* OMPs, included OprH, chaperone GroEL, ribosomal protein L25, and four hypothetical proteins including PA4824 were increased at the outer membrane during growth in low magnesium (Figure 3). Furthermore, transcriptional profiling analysis confirmed increased expression of genes encoding OprH and PA4824 during growth of *P. aeruginosa* in low magnesium. OprH is an outer membrane protein previously shown to be induced by magnesium stress and regulated by PhoP [11]. Although highly abundant, OprH was not identified in the course of ICAT analysis due to its lack of cysteine. Interestingly, cytoplasmic proteins GroEL and ribosomal protein L25 were also increased at the outer membrane fraction during magnesium limitation (Figure 3) corroborating results from ICAT analysis (see above). In the bacterial cell, gene expression and protein synthesis are temporally and spatially coupled with

protein export. *Escherichia coli* membrane-associated polysomes almost exclusively translate membrane and transported proteins whereas cytoplasmic proteins are typically synthesized by the cytoplasmic polysomes [32]. The intracellular "shift" of ribosomal components to the envelope fraction suggests that the majority of protein synthesis occurs at the cytoplasmic membrane during *P. aeruginosa* growth in low magnesium. This likely enables the extensive envelope remodeling characteristic of the response to this environmental stress [33, 10].

Conclusions

Results of this and another study [34] demonstrated the utility of large-scale quantitative proteomic approach such as ICAT reagent-labeling and automated tandem mass spectrometry for the functional analysis of whole bacteria. All previously defined *P. aeruginosa* magnesium-stress response proteins were identified, confirming the validity of this approach. Furthermore, this study demonstrated that even small changes in protein abundance could have significant biological effects. Changes in *P. aeruginosa* subcellular protein compartmentalization due to environmental stress were also observed. Though this data warrants caution during interpretation of the protein abundance based on the analysis of individual subcellular fractions, it also indicates the validity of quantitative proteomic approaches in the definition of change in the protein subcellular localization as a mechanism for the posttranslational protein regulation [35]. Therefore, quantitative proteomic technology can be successfully applied to the analysis of whole bacteria and to the discovery of functionally relevant biologic phenotypes.

Acknowledgments

The authors thank Greg Niemi and Richard Newitt for help in assembling a functional μLC-ESI-MS/MS system, Samuel Donohue and Michael Wright for help with protein labeling protocol, and Priska Von Haller for help with data organization and analysis. This work was supported by grants from the Cystic Fibrosis Foundation (MILLER00P0) and NIH R01 (AI47938) to SIM, and by NIH (R33CA93302-01) to DG and RA. The project has been funded in part with Federal funds from the National Heart Lung and Blood Institute, NIH, under contract no. NO1-HV-28179.

References

1. Griffin, T. J.; Gygi, S. P.; Ideker, T.; Rist, B.; Eng, J.; Hood, L.; Aebersold, R. Complementary Profiling of Gene Expression at the Transcriptome and Proteome Levels in Saccharomyces cerevisiae. *Mol. Cell Proteom* **2002,** *1,* 323–333.
2. Gygi, S. P.; Rochon, Y.; Franza, B. R.; Aebersold, R. Correlation Between Protein and mRNA Abundance in Yeast. *Mol. Cell Biol* **1999,** *19,* 1720–1730.
3. Ideker, T.; Thorsson, V.; Ranish, J. A.; Christmas, R.; Buhler, J.; Eng, J. K.; Bumgarner, R.; Goodlett, D. R.; Aebersold, R.; Hood, L. Integrated Genomic and Proteomic Analyses of a Systematically Perturbed Metabolic Network. *Science* **2001,** *292,* 929–934.
4. Gygi, S. P.; Corthals, G. L.; Zhang, Y.; Rochon, Y.; Aebersold, R. Evaluation of Two-Dimensional Gel Electrophoresis-Based Proteome Analysis Technology. *Proc. Natl. Acad. Sci. U.S.A* **2000,** *97,* 9390–9395.
5. Han, D. K.; Eng, J.; Zhou, H.; Aebersold, R. Quantitative Profiling of Differentiation-Induced Microsomal Proteins Using Isotope-Coded Affinity Tags and Mass Spectrometry. *Nat. Biotechnol* **2001,** *19,* 946–951.
6. Gygi, S. P.; Rist, B.; Gerber, S. A.; Turecek, F.; Gelb, M. H.; Aebersold, R. Quantitative Analysis of Complex Protein Mixtures Using Isotope-Coded Affinity Tags. *Nat. Biotechnol* **1999,** *17,* 994–999.
7. Bodey, G. P.; Bolivar, R.; Fainstein, V.; Jadeja, L. Infections Caused by Pseudomonas aeruginosa. *Rev. Infect. Dis* **1983,** *5,* 279–313.
8. Davis, P. B.; Drumm, M.; Konstan, M. W. Cystic Fibrosis. *Am. J. Respir. Crit. Care Med* **1996,** *154,* 1229–1256.
9. Burns, J. L.; Gibson, R. L.; McNamara, S.; Yim, D.; Emerson, J.; Rosenfeld, M.; Hiatt, P.; McCoy, K.; Castile, R.; Smith, A. L.; Ramsey, B. W. Longitudinal Assessment of Pseudomonas aeruginosa in Young Children with Cystic Fibrosis. *J. Infect. Dis* **2001,** *183,* 444–452.
10. Ernst, R. K.; Yi, E. C.; Guo, L.; Lim, K. B.; Burns, J. L.; Hackett, M.; Miller, S. I. Specific Lipopolysaccharide Found in Cystic Fibrosis Airway Pseudomonas aeruginosa. *Science* **1999,** *286,* 1561–1565.
11. Macfarlane, E. L.; Kwasnicka, A.; Ochs, M. M.; Hancock, R. E. PhoP-PhoQ homologues in Pseudomonas aeruginosa Regulate Expression of the Outer-Membrane Protein OprH and Polymyxin B Resistance. *Mol. Microbiol* **1999,** *34,* 305–316.
12. Hajjar, A. M.; Ernst, R. K.; Tsai, J. H.; Wilson, C. B.; Miller, S. I. Human Toll-Like Receptor 4 Recognizes Host-Specific LPS Modifications. *Nat. Immunol* **2002,** *3,* 354–359.
13. Singh, P. K.; Schaefer, A. L.; Parsek, M. R.; Moninger, T. O.; Welsh, M. J.; Greenberg, E. P. Quorum Sensing Signals Indicate that Cystic Fibrosis Lungs are Infected with Bacterial Biofilms. *Nature* **2000,** *407,* 762–764.
14. Garcia-Vescovi, E.; Soncini, F. C.; Groisman, E. A. Mg2+ as an Extracellular Signal: Environmental Regulation of Salmonella virulence. *Cell* **1996,** *84,* 165–174.
15. Yi, E. C.; Marelli, M.; Lee, H.; Purvine, S. O.; Aebersold, R.; Aitchison, J. D.; Goodlett, D. R. Approaching Complete Peroxisome Characterization by Gas-Phase Fractionation. *Electrophoresis* **2002,** *23,* 3205–3216.
16. von Haller, P. D.; Donohoe, S.; Goodlett, D. R.; Aebersold, R.; Watts, J. D. Mass Spectrometric Characterization of Proteins Extracted from Jurkat T Cell Detergent-Resistant Membrane Domains. *Proteomics* **2001,** *1,* 1010–1021.
17. Guina, T.; Yi, E. C.; Wang, H.; Hackett, M.; Miller, S. I. A PhoP-Regulated Outer-Membrane Protease of Salmonella typhimurium Promotes Resistance to α-Helical Antimicrobial Peptides. *J. Bacteriol* **2000,** *182,* 4077–4086.
18. Calfee, M. W.; Coleman, J. P.; Pesci, E. C. Interference with Pseudomonas quinolone Signal Synthesis Inhibits Virulence Factor Expression by Pseudomonas aeruginosa. *Proc. Natl. Acad. Sci. U.S.A* **2001,** *98,* 11633–11637.
19. Pesci, E. C.; Milbank, J. B.; Pearson, J. P.; McKnight, S.; Kende, A. S.; Greenberg, E. P.; Iglewski, B. H. Quinolone Signaling in the Cell-to-Cell Communication System of Pseudomonas aeruginosa. *Proc. Natl. Acad. Sci. U.S.A* **1999,** *96,* 11229–11234.
20. Johnson, C. R.; Newcombe, J.; Thorne, S.; Borde, H. A.; Eales-Reynolds, L. J.; Gorringe, A. R.; Funnell, S. G.; McFadden, J. J. Generation and Characterization of a PhoP Homologue Mutant of Neisseria meningitidis. *Mol. Microbiol* **2001,** *39,* 1345–1355.

21. Gunn, J. S.; Lim, K. B.; Krueger, J.; Kim, K.; Guo, L.; Hackett, M.; Miller, S. I. PmrA-PmrB-Regulated Genes Necessary for 4-Aminoarabinose Lipid A Modification and Polymyxin Resistance. *Mol. Microbiol* **1998,** *27,* 1171–1182.
22. Guo, L.; Lim, K. B.; Poduje, C. M.; Daniel, M.; Gunn, J. S.; Hackett, M.; Miller, S. I. Lipid A Acylation and Bacterial Resistance Against Vertebrate Antimicrobial Peptides. *Cell* **1998,** *95,* 189–198.
23. Guo, L.; Lim, K. B.; Gunn, J. S.; Bainbridge, B.; Darveau, R. P.; Hackett, M.; Miller, S. I. Regulation of Lipid A Modifications by Salmonella typhimurium Virulence Genes phoP-phoQ. *Science* **1997,** *276,* 250–253.
24. Davies, D. G.; Parsek, M. R.; Pearson, J. P.; Iglewski, B. H.; Costerton, J. W.; Greenberg, E. P. The Involvement of Cell-to-Cell Signals in the Development of a Bacterial Biofilm. *Science* **1998,** *280,* 295–298.
25. Erickson, D. L.; Endersby, R.; Kirkham, A.; Stuber, K.; Vollman, D. D.; Rabin, H. R.; Mitchell, I.; Storey, D. G. Pseudomonas aeruginosa Quorum Sensing Systems May Control Virulence Factor Expression in the Lungs of Patients with Cystic Cibrosis. *Infect. Immun* **2002,** *70,* 1783–1790.
26. Middleton, B.; Rodgers, H. C.; Camara, M.; Knox, A. J.; Williams, P.; Hardman, A. Direct Detection of N-acylhomoserine Lactones in Cystic Fibrosis Sputum. *FEMS Microbiol. Lett* **2002,** *207,* 1–7.
27. Pearson, J. P.; Gray, K. M.; Passador, L.; Tucker, K. D.; Eberhard, A.; Iglewski, B. H.; Greenberg, E. P. Structure of the Autoinducer Required for Expression of Pseudomonas aeruginosa Virulence Genes. *Proc. Natl. Acad. Sci. U.S.A* **1994,** *91,* 197–201.
28. van Delden, C.; Comte, R.; Bally, A. M. Stringent Response Activates Quorum Sensing and Modulates Cell Density-Dependent Gene Expression in Pseudomonas aeruginosa. *J. Bacteriol* **2001,** *183,* 5376–5384.
29. Whiteley, M.; Parsek, M. R.; Greenberg, E. P. Regulation of Quorum Sensing by RpoS in Pseudomonas aeruginosa. *J. Bacteriol* **2000,** *182,* 4356–4360.
30. D'Argenio, D. A.; Calfee, M. W.; Rainey, P. B.; Pesci, E. C. Autolysis and Autoaggregation in Pseudomonas aeruginosa Colony Morphology Mutants. *J. Bacteriol* **2002,** *184,* 6481–6489.
31. Gallagher, L. A.; McKnight, S. L.; Kuznetsova, M. S.; Pesci, E. C.; Manoil, C. Functions Required for Extracellular Quinolone Signaling by Pseudomonas aeruginosa. *J. Bacteriol* **2002,** *184,* 6472–6480.
32. Randall, L. L.; Hardy, S. J. Synthesis of Exported Proteins by Membrane-Bound Polysomes Form Escherichia coli. *Eur. J. Biochem* **1977,** *75,* 43–53.
33. Bell, A.; Hancock, R. E. Outer Membrane Protein H1 of Pseudomonas aeruginosa: Purification of the Protein and Cloning and Nucleotide Sequence of the Gene. *J. Bacteriol* **1989,** *171,* 3211–3217.
34. Baliga, N. S.; Pan, M.; Goo, Y. A.; Yi, E. C.; Goodlett, D. R.; Dimitrov, K.; Shannon, P.; Aebersold, R.; Ng, W. V.; Hood, L. Coordinate Regulation of Energy Transduction Modules in Halobacterium sp. Analyzed by a Global Systems Approach. *Proc. Natl. Acad. Sci. U.S.A* **2002,** *99,* 14913–14918.
35. Shapiro, L.; McAdams, H. H.; Losick, R. Generating and Exploiting Polarity in Bacteria. *Science* **2002,** *298,* 1942–1946.